Original Article
EIF3H interacts with PDCD4 enhancing lung adenocarcinoma cell metastasis

Yingying Hu[1*], Xiao Wei[1*], Yumin Lv[1*], Xin Xie[1], Liu Yang[1], Jingjing He[1], Xingyu Tao[1], Yuting Ma[1], Yun Su[1], Liyang Wu[1], Weiyi Fang[2], Zhen Liu[1]

[1]Affiliated Cancer Hospital & Institute of Guangzhou Medical University, Guangzhou Municipal and Guangdong Provincial Key Laboratory of Protein Modification and Degradation, State Key Laboratory of Respiratory Disease, School of Basic Medical Sciences, Guangzhou Medical University, Guangzhou 510095, Guangdong, P. R. China; [2]Cancer Institute, Southern Medical University, Guangzhou 510515, Guangdong, P. R. China. *Equal contributors.

Abstract: Lung adenocarcinoma (LUAD) is a common type of lung cancer characterized by a high incidence of local invasion and metastasis. Programmed cell death factor 4 (PDCD4) is a well-recognized tumor suppressor gene involved in LUAD, however its precise regulatory mechanism remains elusive. This is the first study to report an inverse regulatory relationship between PDCD4 and eukaryotic translation initiation factor 3 subunit H (EIF3H) in LUAD. Co-immunoprecipitation assays combined with mass spectrometry and immunofluorescent co-localization indicated that PDCD4 interacted with EIF3H. Overexpression of PDCD4 in LUAD cells reduced EIF3H mRNA and protein levels by suppressing c-Jun-induced EIF3H transcription. Further, an elevated level of EIF3H protein was found in LUAD tissues compared with para-cancerous normal lung tissues, and was found to be an unfavorable factor promoting LUAD pathogenesis. Moreover, the negative correlation between PDCD4 and EIF3H protein expression was confirmed in LUAD tissues. Functional analyses showed that EIF3H overexpression promoted LUAD cell migration and invasion in vitro as well as metastasis in nude mice by activating epithelial-mesenchymal transition (EMT) signaling. Conversely, EIF3H knockdown with small interfering RNAs reversed these changes in LUAD cells. Furthermore, we discovered that introduction of PDCD4 to EIF3H-overexpressing LUAD cells abrogated the function of EIF3H, reducing migration and invasion of LUAD cells by downregulating EMT signaling. Taken together, our findings identified a previously unknown negative regulation of PDCD4 on EIF3H and confirmed EIF3H as an oncogenic factor in LUAD by enhancing EMT signaling, which was abrogated by PDCD4.

Keywords: Lung adenocarcinoma, EIF3H, PDCD4, metastasis, invasion

Introduction

Lung cancer is the leading cause of cancer-related mortality worldwide, accounting for approximately 1.8 million deaths in 2012 [1], and continued to be the most frequently diagnosed cancer (11.6% of the total cases) in 2018 [2]. Non-small cell lung cancer (NSCLC) comprises more than 85% of lung cancers, among which adenocarcinoma accounts for approximately 40% of cases [3]. The majority of patients diagnosed with lung adenocarcinoma (LUAD) present with locally advanced or metastatic disease, with recurrence and metastasis being quite common, even at early stages of development [4]. Despite the use of cytotoxic chemotherapies and molecular-targeting thera-

pies, the 5-year survival rate of patients diagnosed at late-stage is still poor due to local invasion and distant metastases [5, 6].

Programmed cell death factor 4 (PDCD4) is a well-studied tumor suppressor involved in different types of cancer. It suppresses tumor progression, gene transcription, protein translation, and also induces apoptosis [7-9]. Increased PDCD4 expression has been shown to inhibit tumorigenesis in a transgenic mouse model and in nude mice, and attenuate tumor cell invasion in vitro [10-13]. PDCD4 mRNA and protein levels are significantly decreased in LUAD tissues, and reduced PDCD4 expression is positively correlated with increased grade/disease stage and poor prognosis of patients [14].

Table 1. Characteristics of lung adenocarcinoma patients from TCGA dataset

Characteristic	NO. of patients (n=522)	%
Gender		
Male	242	46.4
Female	280	53.6
Age		
≤50	38	7.27
>50	465	89.1
unknown	19	3.63
Clinical stage		
I	279	53.4
II	124	23.8
III	85	16.3
IV	26	4.98
unknown	8	1.53
N stage		
N_0	335	64.2
N_1	98	18.8
N_2	75	14.4
N_3	2	0.38
N_x	11	2.11
unknown	1	0.19
T stage		
T_1	172	33.0
T_2	281	53.8
T_3	47	9.00
T_4	19	3.64
T_x	3	0.57
M stage		
M_0	353	67.6
M_1	25	4.79
M_x	140	26.8
unknown	4	0.77

However, the proteins that interact with PDCD4, as well as their specific mechanisms in LUAD metastasis have not yet been fully studied.

Our study aims to investigate the potential mechanisms of the anti-metastatic function of PDCD4 in LUAD. Here, results of co-immuno-precipitation, mass spectrometry, and immuno-fluorescent co-localization showed that PDCD4 interacts with EIF3H in LUAD. EIF3H expression was upregulated in LUAD cells and tissues compared with immortalized human bronchial epithelial cells and para-cancerous normal lung tissues, respectively. EIF3H protein expression level was negatively correlated with PDCD4

level in human LUAD. In addition, EIF3H overexpression significantly induced LUAD cell migration and invasion *in vitro* and metastasis *in vivo*, whereas EIF3H knockdown produced the opposite effect. Mechanistically, EIF3H activated EMT signaling by increasing fibronectin, N-cadherin, β-catenin, vimentin, and snail expression, as well as by suppressing E-cadherin. The modulatory relationship between PDCD4 and EIF3H was further explored. PDCD4 suppressed the mRNA and protein expression of EIF3H by negatively regulating c-Jun, which was a transcriptional promotor of EIF3H. The introduction of PDCD4 to EIF3H-overexpressing LUAD cells abrogated cell migration and invasion by inactivating EMT signaling. These results suggest that EIF3H is a novel candidate oncogenic factor and a potential therapeutic target participating in PDCD4 modulated anti-metastatic function in LUAD.

Materials and methods

Analysis of LUAD data from TCGA

LUAD mRNA expression profiles were studied using HTSeq-Count normalized RNA-Seq values from normal solid tissue specimens and primary tumors obtained from The Cancer Genome Atlas database (TCGA). RNA-Seq data from 535 LUAD tissue samples and 59 normal lung tissue samples were collected and 522 out of 535 LUAD patients had complete survival data. Various clinicopathological parameters, including clinical stage, T stage, N stage, M stage and overall survival time (OS) were also downloaded and assessed. Patients with unknown clinical information were excluded. The various characteristics of LUAD patients are shown in **Table 1**.

Tissue array specimens

Tissue microarrays of LUAD (n=83) and para-cancerous normal tissues (n=77) were purchased from Shanghai Outdo Biotech Co. Ltd. (Shanghai, China). The patient characteristics are shown in **Table 2**.

Cell culture

SPCA-1, A549, H322, H1299 and H1975 lung cancer cell lines were purchased from the Shanghai Cell Bank of the Chinese Academy of Sciences, China. These cells were cultured in RPMI 1640 supplemented with 10% fetal

Table 2. Characteristics of lung adenocarcinoma patients in tissue array

Characteristic	NO. of patients (n=83)	%
Gender		
Male	44	53.0
Female	39	47.0
Age		
≤50	10	12.0
>50	73	88.0
Clinical stage		
I-II	46	55.4
III-IV	34	41.0
unknown	3	3.6
N stage		
N_0-N_1	55	66.3
N_2-N_3	15	18.1
unknown	13	15.6
T stage		
T_1-T_2	62	74.7
T_3-T_4	21	25.3

bovine serum (FBS) (PAN, Adenbach, Germany) at 37°C in a humidified atmosphere of 5% CO_2. The 16HBE immortalized human bronchial epithelial cell line was obtained from the Pathology Department, School of Basic Medical Sciences, Guangzhou Medical University, Guangzhou, China and cultured in DMEM supplemented with 10% fetal bovine serum (FBS) (PAN, Adenbach, Germany).

Lentivirus infection

Lentiviral particles encoding FLAG-tagged EIF3H (GV358-EIF3H vector, LV) and its control sequence (NC) were designed and constructed by GeneChem (Shanghai, China). Both lentiviral particles expressed green fluorescent protein (GFP). In brief, A549 and H322 cells were seeded in 24-well plates at a density of 5000 cells per well. Lentiviral particles were added to the cells at 50-60% confluency, and the cells were incubated at 37°C for 10 h. The cells expressing GFP were observed under an Olympus fluorescent microscope (Tokyo, Japan) at 72 h after infection, and the efficiency of the lentiviral infection was quantitatively assessed by western blot and RT-qPCR.

Cell transfection

The FLAG-tagged pENTER-PDCD4 plasmids with puromycin resistance were purchased

from Vigene Biosciences (Shangdong, China). Cells in the exponential phase of growth were seeded in 6-well plates at a density of $2×10^5$ cells per well for transfection. The plasmids were co-transfected into cells at 40-60% confluency using Lipofectamine 3000 (Invitrogen Biotechnology Co., Ltd., Shanghai, China) according to the manufacturer's instructions. At 8 h after transfection, the medium was replaced. Efficiency of the transfection was quantitatively assessed by Western blot and RT-qPCR at 48 h after transfection.

Western blot analyses

Whole proteins were extracted in RIPA lysis buffer supplemented with phosphatase and protease inhibitors (Beyotime Institute of Biotechnology, Shanghai, China), and protein concentrations were quantified with the BCA Protein Assay (Thermo Scientific, Waltham, MA, USA). The proteins were separated by 10% SDS-PAGE and then transferred onto polyvinyldifluoride membranes (EMD Millipore, Billerica, MA, USA), followed by incubation with primary antibodies overnight. Primary antibodies used: anti-PDCD4 (CST 9535S, 1:1000 dilution), anti-EIF3H (CST 3413S, 1:1000 dilution), anti-c-Jun (CST 9165, 1:1000 dilution), anti-Flag (Sigma F1804, 1:1000 dilution), anti-β-catenin (Proteintech 51067-2-AP, 1:1000 dilution), anti-vimentin (Proteintech 10366-1-AP, 1:1000 dilution), anti-N-ca (Proteintech 66219-1-Ig, 1:1000 dilution), anti-E-ca (Proteintech 60335-1-Ig, 1:1000 dilution), anti-snail (CST 3879S, 1:1000 dilution), anti-GAPDH (Bioworld AP-0063, 1:10000 dilution), anti-tubulin (CWBIO CW0098, 1:2000 dilution), anti-β-actin (CWBIO CW0096, 1:2000 dilution).

RT-qPCR

Total RNA was isolated with TRIzol Reagent (Takara Bio, Inc., Otsu, Japan) and reverse transcribed into cDNA with the PrimeScript Kit (Takara Bio, Inc.) according to the manufacturer's instructions. cDNA was then used as a template for quantitative reverse transcription polymerase chain reactions (RT-qPCR). GAPDH was used as the internal control, and the relative changes between two groups were analyzed by the $2^{-\Delta\Delta Ct}$ method. The primers used were as follows: PDCD4 (forward, 5'-ATGTGGAGG-AGGTGGATGTG-3'; reverse 5'-TGGTGTTAAAG-TCTTCTCAAATGC-3'), EIF3H (forward, 5'-CAGA-

TGGAAATGATGCGGAGC-3'; reverse 5'-AGTAT-GTGGACTGATACCAGCC-3'), and GAPDH (forward, 5'-CGGAGTCAACGGATTTGGTCGTAT-3'; reverse, 5'-AGCCTTCTCCATGGTGGTGAAGAC-3'). Each sample was amplified in triplicate in independent reactions.

Co-immunoprecipitation (CoIP)

Co-IP was performed with the Pierce Co-Immunoprecipitation Kit (Thermo Scientific) according to the manufacturer's instructions. In brief, total proteins were extracted from cells, and the amount of protein was quantified. After coupling the affinity-purified PDCD4 (CST 9535S) or EIF3H (CST 3413S) antibody to amine- and carrier protein-free beads, proteins were incubated with the beads overnight at 4°C. The proteins were pulled down with elution buffer, the samples were centrifuged, and the supernatant was collected. The samples were analyzed by mass spectrometry and Western blot. Anti-IgG (CST 2729S) was used as the negative control.

Chromatin immunoprecipitation assay (ChIP)

ChIP was performed with a Chromatin Immunoprecipitation Kit (Thermo Scientific) according to the manufacturer's instructions. DNA-protein complexes were immunoprecipitated from A549 cells using a c-Jun antibody (CST 9165), with normal mouse IgG (CST 2729S) as a negative control. Specific primers (primer 1: forward, 5'-TTTCATAAAGAGGGCCCACATG-AA-3'; reverse, 5'-ACTAGGTAGCTGGAATGATG-AGCA-3'. primer 2: forward, 5'-TGGAAAACA-GGAGGGAGGCG-3'; reverse, 5'-CGTGAGTTAC-CGGAAGCGGA-3'. primer 3: forward, 5'-ACA-CCATTGCACTCCAGCCT-3'; reverse, 5'-AGACT-TTGAACATCTTCTTTCCCCT-3') were utilized to amplify the EIF3H promoter region.

Cell migration and invasion assays

For the cell migration assay, transwell chambers with polycarbonate membrane filters (pore size, 8 μm; BD Biosciences, San Jose, CA, USA) were used. Approximately 0.1 ml of serum-free RPMI 1640 containing 5×10^5 LUAD cells were added to the upper chamber and 0.6 ml of RPMI 1640 supplemented with 10% FBS were added to the lower chamber. At 16-24 h after incubation, the cells that had migrated through the membrane were fixed in paraformaldehyde and stained with Giemsa (Beyotime Institute of Biotechnology). The number of migrated cells in three randomly selected fields was counted under an Olympus microscope and then the values were averaged. For the invasion assay, the transwell chambers were coated with 50 μl of 1:4-diluted Matrigel (Matrigel: RPMI 1640). Approximately 0.1 ml of serum-free RPMI 1640 containing 5×10^5 cells was added to the upper chamber, and 0.6 ml of RPMI 1640 supplemented with 10% FBS was added to the lower chamber. At 30 h after incubation, the cells that had invaded the Matrigel and migrated through the membrane were fixed with paraformaldehyde and stained with Giemsa. The number of invasive cells in three randomly selected fields was counted under an Olympus microscope and then the values were averaged.

Immunofluorescence

The cells were seeded on coverslips in 24-well format and cultured overnight to facilitate attachment. After fixing in 4% paraformaldehyde, the cells were permeabilized in 0.2% Triton X-100 and then incubated with the indicated antibody overnight at 4°C. Cell nuclei were counterstained with 0.1 ml of DAPI (0.2 mg/ml), and the cells were visualized under a confocal microscope (Carl Zeiss, Germany).

Immunohistochemistry (IHC)

The paraffin-embedded sections were deparaffinized and hydrated, followed by the retrieval of antigens and blocking of endogenous peroxidase activity. The sections were incubated with antibody against PDCD4 (CST 9535S, 1:200 dilution) or EIF3H (CST 3413S, 1:200 dilution). Overnight at 4°C. After washing, the sections were incubated with a horseradish peroxidase (HRP)-conjugated secondary antibody, and the stain was developed with DAB (Maixin Biotech. Co., Ltd., Fuzhou, China). The staining intensity was defined as 0 (no reactivity), 1 (light yellow), 2 (yellowish-brown), or 3 (brown). Areas of staining were classified according to the percentage of positive cells: 1 if ≤10%, 2 if 11-50%, and 3 if ≥51%. The staining intensity and the percentage score were multiplied to obtain the total score. Total scores ≥3 indicated positive results (0-4 was defined as low expression and ≥5 as high expression).

Xenograft mice model

Animal experiments were approved by the Institutional Animal Ethical Committee, Experimental Animal Center of Guangzhou Medical University, China. A pulmonary metastasis model was established to carry out the metastasis assays. Briefly, approximately 5×10^6 A549 cells were injected into the tail vein of 4-5 week old BALB/c-nu mice (n=5 per group). The animals were sacrificed at 30 days after injection, and the formation of metastatic lesions was evaluated using fluorescence microscopy.

Statistical analysis

Statistical analyses were performed using SPSS 21.0 software (SPSS Inc. Chicago, IL, USA). Statistical significance between two groups was determined by Student's two-tailed *t*-test. The correlation between gene expression and clinicopathological features was analyzed by the chi-square test. The relationship between PDCD4 and EIF3H was confirmed by Spearman's correlation analysis. Kaplan-Meier analysis, based on the TCGA database, was performed using the survival R package. *P*-values <0.05 were considered to be statistically significant.

Results

PDCD4 interacted with EIF3H in LUAD cells

After transiently transfecting FLAG-tagged pEN-TER-PDCD4 plasmids into SPCA-1 cells (**Figure 1A**), co-immunoprecipitation (CoIP) was performed to identify the proteins interacting with PDCD4. As shown in **Figure 1B**, a specific target band of approximately 60-63 kDa was identified and then excised from the gel for protein identification by mass spectrometry. A total of 327 predicted candidate proteins were identified by mass spectrometry. Proteins with low mass spectrometry scores (less than 100) were ruled out because of their weak interactions with PDCD4. The screening range was subsequently narrowed down by excluding the proteins which were predicted to display different subcellular localization from PDCD4. EIF3H, a protein subunit of translation initiation factor eIF3 was discovered with a mass spectrometry score of 202 and the similar predicted localization to PDCD4 (in the nucleus and cytoplasm). Exogenous CoIP assays were conducted to con-

firm binding between PDCD4 and EIF3H. After transfection of FLAG-tagged pENTER-PDCD4 plasmids into SPCA-1 cells (**Figure 1Ci**), EIF3H, but not IgG, was pulled down after incubation with anti-EIF3H antibody (**Figure 1Di**). The interaction between PDCD4 and EIF3H was further confirmed by inverse co-immunoprecipitation. After transfection of FLAG-tagged GV358-EIF3H plasmids into SPCA-1 cells (**Figure 1Cii**), PDCD4, but not IgG, was pulled down after incubation with anti-PDCD4 antibody (**Figure 1Dii**). In addition, double immunofluorescent staining confirmed the co-localization of PDCD4 and EIF3H proteins in the nucleus and cytoplasm of SPCA-1 cells (**Figure 1E**). These results indicated that PDCD4 interacted with EIF3H in LUAD.

PDCD4 negatively regulated EIF3H in LUAD

To investigate the regulatory relationship between PDCD4 and EIF3H, pENTER-PDCD4 plasmid was transiently transfected into H1299 and SPCA-1 cells to overexpress PDCD4. As shown in **Figure 2A**, PDCD4 protein expression was increased in both H1299 and SPCA-1 cells. In contrast, EIF3H protein level was reduced after PDCD4 overexpression (**Figure 2A**). Furthermore, EIF3H mRNA expression in PD-CD4-overexpressed cells was almost 4 times lower than in the control cells (**Figure 2B**). These results indicated that PDCD4 negatively regulated EIF3H at the transcriptional level in LUAD. However, the reverse as not true, EIF3H had no influence on PDCD4 protein expression (**Figure 2C**).

To further explore the mechanisms by which PDCD4 regulated EIF3H in LUAD, the JASPAR database was used to analyze a 2-kb region upstream of the transcription start site of EIF3H. Three c-Jun-binding motifs at -274 to -286, -1949 to -1961 and -1353 to -1366 were predicted inside the EIF3H promoter region (**Figure 2D**). RT-qPCR and Western blot demonstrated that both mRNA and protein levels of EIF3H were elevated after the transfection of c-Jun plasmids, suggesting c-Jun as an upstream regulator of EIF3H (**Figure 2E**). Interestingly, c-Jun and EIF3H were both decreased in PDCD4 overexpressing LUAD cells and further co-transfection with c-Jun abrogated the inhibitory effect of PDCD4 on EIF3H, indicating that PDCD4 negatively regulated
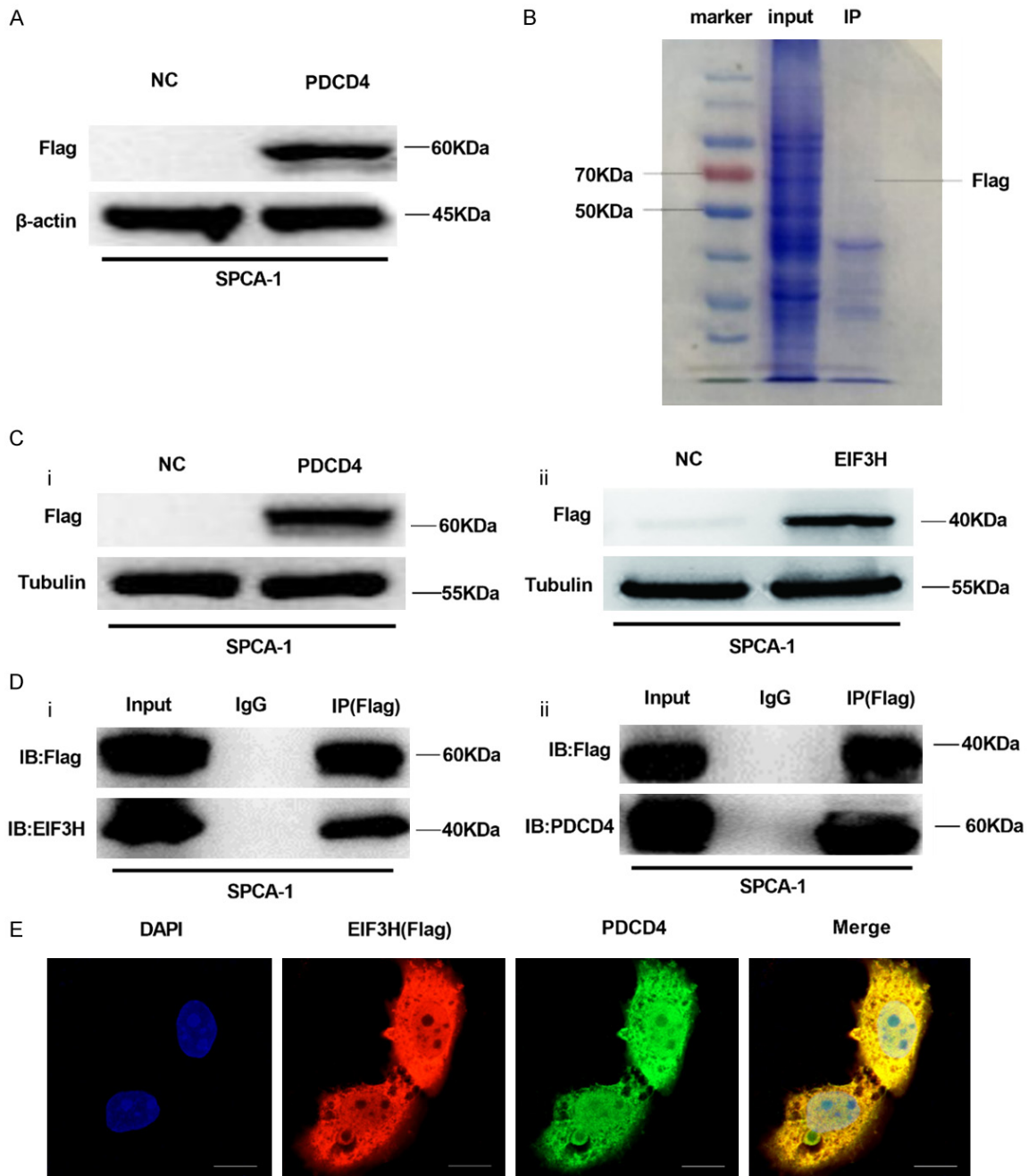
Figure 1. PDCD4 interacted with EIF3H in LUAD cells. A. Overexpression of PDCD4 in SPCA-1 cells after transfection of the FLAG-tagged pENTER-PDCD4 plasmid was confirmed by Western blot. B. After incubation with the anti-Flag antibody, co-immunoprecipitation, Western blot and Coomassie brilliant blue staining were performed using PDCD4-overexpressing cell lysates. Input served as the positive control. C. Overexpression of PDCD4 or EIF3H in SPCA-1 cells after transfection with (i) FLAG-tagged pENTER-PDCD4 or (ii) FLAG-tagged GV358-EIF3H plasmid was confirmed by Western blot. D. Binding between PDCD4 and EIF3H was verified by co-immunoprecipitation. PDCD4 overexpressing or EIF3H overexpressing cell lysates were respectively immunoprecipitated with anti-Flag antibody and immunoblotted with either (i) anti-EIF3H or (ii) anti-PDCD4 antibody. Input served as the positive control and IgG as the negative control. E. Co-localization of EIF3H with PDCD4. Immunofluorescent signals for PDCD4 (green) and EIF3H (red) distributed in the nucleus and cytoplasm of SPCA-1 cells. The yellow signal indicated co-localization. Scale bar: 10 μm.

EIF3H by decreasing expression of c-Jun (**Figure 2F**). ChIP and qPCR assays further confirmed that c-Jun directly bound to the -1353~-1366 site of the EIF3H promoter in LUAD cells, and
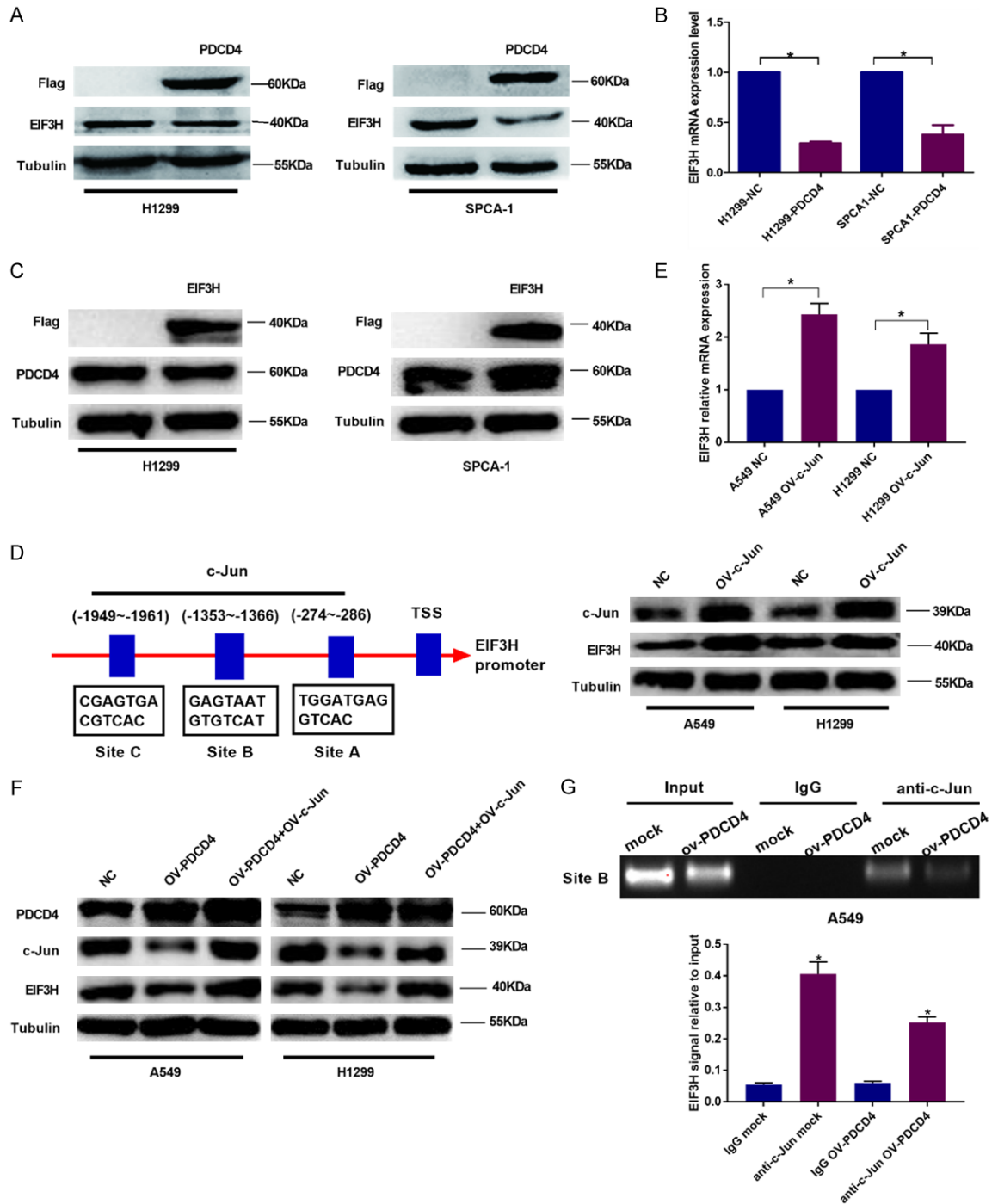
Figure 2. PDCD4 negatively regulates EIF3H in LUAD. (A) Western blot and (B) RT-qPCR analysis of EIF3H protein and mRNA expression after transfection of FLAG-tagged PDCD4 in LUAD cell lines H1299 and SPCA-1. Student's t-test, mean ± S.E, *P<0.05. (C) Western blot analysis of PDCD4 protein expression after EIF3H overexpression in LUAD cell lines. (D) Potential c-Jun binding sites on the EIF3H promoter were predicted by the JASPER database. (E) Western blot and RT-qPCR analysis of EIF3H expression after c-Jun overexpression. (F) Western blot analysis of EIF3H protein expression after PDCD4 or c-Jun overexpression. (G) Chromatin immunoprecipitation and qPCR to verify the binding of c-Jun on EIF3H.

overexpression of PDCD4 attenuated their binding (**Figure 2G**). Taken together, these find-

ings suggested that PDCD4 suppressed expression of c-Jun to inhibit the transcriptional acti-

vation of EIF3H, subsequently reducing its protein expression.

EIF3H was highly expressed and negatively correlated with PDCD4 expression in human LUAD tissues

For TCGA database analyses, LUAD patients were divided into two groups of EIF3H expression: low and high, with the median mRNA level serving as the cutoff value. The results showed that EIF3H expression was significantly elevated in LUAD tissues compared with normal lung tissues ($P<0.0001$, **Figure 3A**) and that the increased expression of EIF3H in LUAD tissues was strongly associated with poor prognosis of LUAD patients ($P=0.004$, **Figure 3B**). In addition, significantly higher EIF3H expression was found in LUAD patients with advanced clinical stages, large tumor sizes, and distant metastases ($P=0.005$, $P=0.001$, $P=0.000$, respectively, **Figure 3D**).

Next, we evaluated the expression profile of EIF3H protein in LUAD tissues, para-cancerous normal bronchial, and alveolar epithelia by immunohistochemistry (IHC). As shown in **Figure 3D**, EIF3H mainly was expressed in the cytoplasm of LUAD cells and para-cancerous normal epithelial cells with different staining intensities. EIF3H displayed high expression in 60 out of 83 LUAD cases (72.3%), but in only 10 out of 77 para-cancerous tissues (13.0%) ($P<0.01$, **Table 3**), which suggested the upregulation of EIF3H expression in LUAD tissues, in good agreement with results from the TCGA database analysis. Moreover, further analyses of the correlation between EIF3H expression and clinicopathological features also showed significant differences with regard to clinical stage ($P=0.049$) and T stage ($P=0.031$) (**Table 4**). Collectively, EIF3H displayed high expression in LUAD tissues compared to non-cancerous tissues.

Subsequently, the association between PDCD4 and EIF3H was examined in 83 human LUAD specimens by IHC. The results demonstrated that PDCD4 expression was absent or weak in most LUAD tissues, whereas EIF3H expression was strongly expressed (**Figure 3E**). Among 60 LUAD cases with high EIF3H expression, only 2 cases (3.33%) showed high expression of

PDCD4 and 58 cases (96.7%) showed low expression. Among 23 LUAD cases with low EIF3H expression, high PDCD4 expression was observed in 7 cases (30.4%) and low expression was observed in 16 cases (69.6%). Statistical analysis confirmed that there was a negative correlation between the protein expression of PDCD4 and EIF3H in LUAD ($P<0.01$, **Table 5**; **Figure 3F**).

Overexpression of EIF3H promoted cell migration and invasion in LUAD by activating the EMT pathway

Cell experiments were performed to further explore the role of EIF3H in LUAD. EIF3H protein level was measured in human immortalized bronchial epithelial cells (16HBE) and five LUAD cell lines. Compared with 16HBE cells, EIF3H expression was significantly elevated in H1299, H332, and H1975 cells and slightly increased in SPCA-1 and A549 cells (**Figure 4A**), which was consistent with our previous results that EIF3H was highly expressed in LUAD tissues. Lentiviral particles encoding FLAG-tagged EIF3H (GV358-EIF3H vector, LV) or its negative control (NC) were introduced into A549 and H322 cells to establish EIF3H stable expressing cell lines A549-EIF3H-LV and H322-EIF3H-LV (**Figure 4B**). After infection, a > 2-fold increase of EIF3H mRNA level was observed in A549-LV and H322-LV cells compared with the control groups (NC). Obvious elevation was also found in A549-LV and H322-LV cells at protein level (**Figure 4C**). Subsequently, cell migration and invasion were detected in EIF3H overexpressing cells by transwell and boyden assays. Transwell assays showed that the number of migrated A549-LV and H322-LV cells was significantly increased compared to control cells (1259±94 vs 574±16 in A549 cells and 427±3 vs 117±10 in H322 cells) ($P<0.05$). Likewise, in Boyden assays, both EIF3H-overexpressed cell lines had significantly more invasive cells compared to negative controls (441±13 vs 296±13 in A549, 243±12 vs 158±14 in H322) ($P<0.05$, **Figure 4D**). Additionally, an *in vivo* pulmonary metastasis model created by intravenous injection of A549-LV or A549-NC cells into BCLC/ nude mice was conducted. Multiple lung metastases were detected in three mice (out of 5) injected with A549-LV cells at day 30, whereas no pulmonary metastasis (0/5) were found in the control group at the same time (**Figure 4E**).
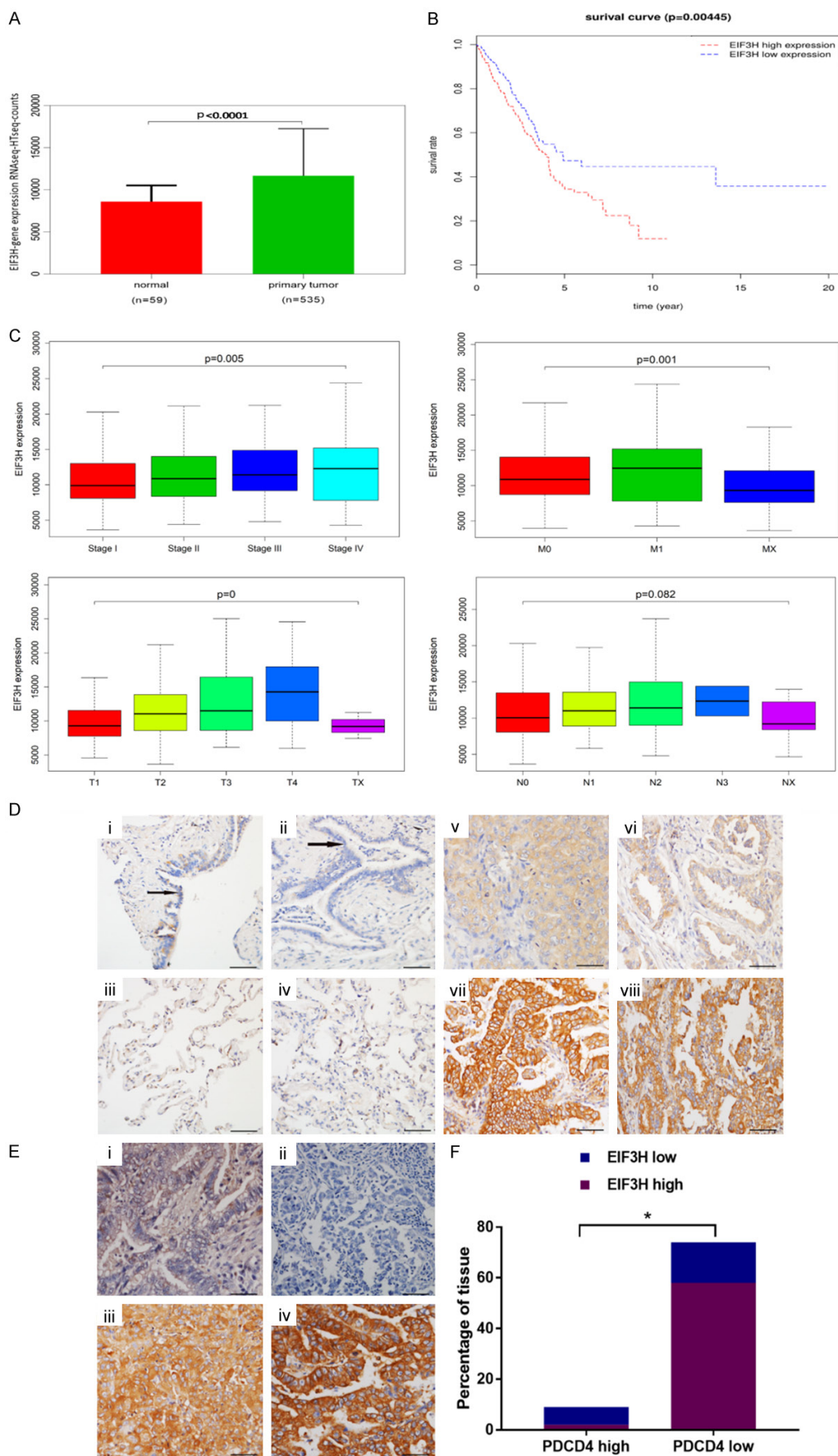
Figure 3. EIF3H showed high expression in LUAD tissues and predicted poor prognosis. A. EIF3H expression was analyzed in 535 LUAD tissues and 59 normal lung tissues. B. Kaplan-Meier curves of OS in LUAD patients. C. LUAD patients were classified according to the clinicopathological features as stage, T, N, and M. Whisker plots are shown from the minimum to the maximum for each group. D. Expression of EIF3H in the para-cancerous normal bronchial epithelium was detected as (i) weak expression and (ii) negative expression. The bronchial epithelium is indicated by the black arrow. Expression of EIF3H in the para-cancerous normal alveolar epithelium was detected as (iii and iv) weak expression. Expression of EIF3H in LUAD tissue was detected as (v and vi) weak expression. Expression of EIF3H in LUAD tissue was detected as (vii and viii) strong expression (DAB/hematoxylin staining, magnification, 200×). Scale bar: 100 μm. E. Expression of EIF3H and PDCD4 in LUAD tissue was detected by immunohistochemistry as (i) weak expression of PDCD4 in LUAD, (ii) negative expression of PDCD4 in LUAD, and (iii and iv) strong expression of EIF3H in LUAD (DAB/hematoxylin staining, magnification of 200×). Scale bar: 100 μm. F. Negative correlation between EIF3H and PDCD4 protein expression in LUAD by Spearman's correlation analysis. *P<0.05.

Table 3. Differentiated expression of EIF3H in lung adenocarcinoma and para-cancerous lung tissues

Group	n	EIF3H expression		χ^2	P value
		high	low		
Cancer	83	60 (72.3%)	23 (27.7%)	57.08	<0.01
Para-cancerous	77	10 (13.0%)	67 (87.0%)		

Table 4. Correlation between EIF3H expression and the clinicopathological features of patients with lung adenocarcinomas

Variables	n	EIF3H expression		χ^2	P value
		high	low		
Age					
≤50	10	8 (80%)	2 (20%)	0.337	0.561
>50	73	52 (71.2%)	21 (28.8%)		
Gender					
Male	44	32 (72.7%)	12 (27.3%)	0.009	0.925
Female	39	28 (71.8%)	11 (28.2%)		
Clinical stage					
I-II	46	32 (69.6%)	14 (30.4%)	0.468	0.049
III-IV	34	26 (76.7%)	8 (23.5%)		
Unknown	3				
T stage					
T_1-T_2	62	41 (66.1%)	21 (33.9%)	4.64	0.031
T_3-T_4	21	19 (90.5%)	2 (9.5%)		
N stage					
N_0-N_1	55	40 (72.7%)	15 (27.3%)	1.245	0.264
N_2-N_3	15	13 (86.7%)	2 (13.3%)		

Table 5. Correlation between protein expression of PDCD4 and EIF3H in lung adenocarcinoma tissues

EIF3H expression	PDCD4 expression	
	high	low
high	2 (3.33%)	58 (96.7%)
low	7 (30.4%)	16 (69.6%)

χ^2=12.63, P<0.01, r=-0.4.

These results confirmed that EIF3H dramatically enhanced LUAD cell migration, invasion and metastasis *in vitro* and *in vivo*.

Next, the mechanisms by which EIF3H promotes LUAD metastasis were explored. After the overexpression of EIF3H in A549 and H322 cells, the levels of EMT-related proteins, including fibronectin, N-cadherin, β-catenin, vimentin, and snail were increased, whereas E-cadherin was decreased, indicating that EIF3H enhanced the metastatic biological behavior by activating EMT signaling in LUAD (**Figure 4F**).

Knockdown of EIF3H attenuated cell migration and invasion in LUAD by inactivating EMT signaling

To further confirm the oncogenic function of EIF3H in LUAD, small interfering RNAs (siRNA) were introduced to knockdown EIF3H expression in H322 and H1299 cells. After this interference, EIF3H mRNA expression and protein level were significantly decreased (**Figure 5A**). Transwell and Boyden assays showed the reduction of migrated and invasive cells in si-EIF3H LUAD cell lines compared to control groups (P<0.05, **Figure 5B**). Mechanistically, protein expression of fibronectin, N-cadherin, β-catenin, vimentin, and snail was reduced, whereas E-cadherin protein expression was elevated in both si-EIF3H groups (**Figure 5C**). Together, knocking down EIF3H reduced both LUAD cell invasiveness and EMT signaling.
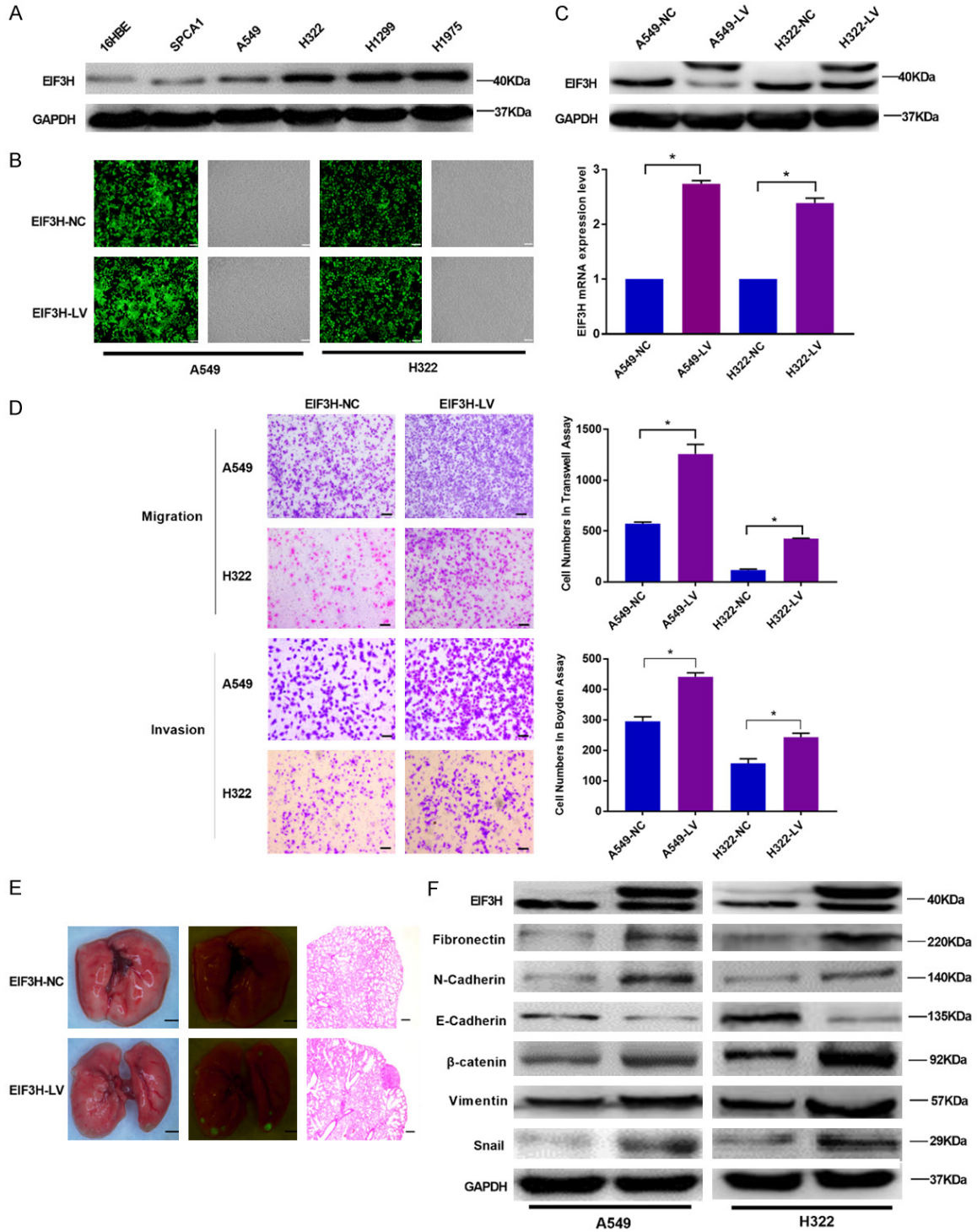
Figure 4. EIF3H promotes cell migration and invasion in LUAD cells. A. Expression of EIF3H in immortal bronchial epithelial cells and LUAD cell lines was detected by Western blotting. B. A549 and H322 cells were infected with the lentivirus encoding FLAG-tagged EIF3H (LV) or control vector (NC). Green fluorescent protein (GFP) expression was used to monitor the infection efficiency. More than 90% of cells showed GFP expression. Scale bar: 100 μm. C. At 48 h after infection, the increased EIF3H protein and mRNA levels were confirmed by Western blotting and RT-qPCR, *P<0.05. D. The effect of EIF3H on cell migration and invasion was determined by transwell and Boyden assays, respectively. Bar graphs represent the average number of cells that passed through the membranes in three independent experiments. Student's t-test, mean ± S.E., *P<0.05. Scale bar: 100 μm. E. Metastasis of EIF3H overexpressing LUAD cells was enhanced in vivo. Nude mice were intravenously injected with EIF3H-overexpressing or control A549 cells (n=5 mice/group) and sacrificed at 30 days after injection. Representative bioluminescent images of the

lungs are shown. Scale bar: 2 mm. Lung metastases were confirmed by H&E staining (100×). Scale bar: 100 µm. F. Expression of EMT-related proteins, namely, fibronectin, N-cadherin, β-catenin, vimentin, snail, and E-cadherin were measured following EIF3H overexpression in A549 and H322 cells. GAPDH was used as the internal control.
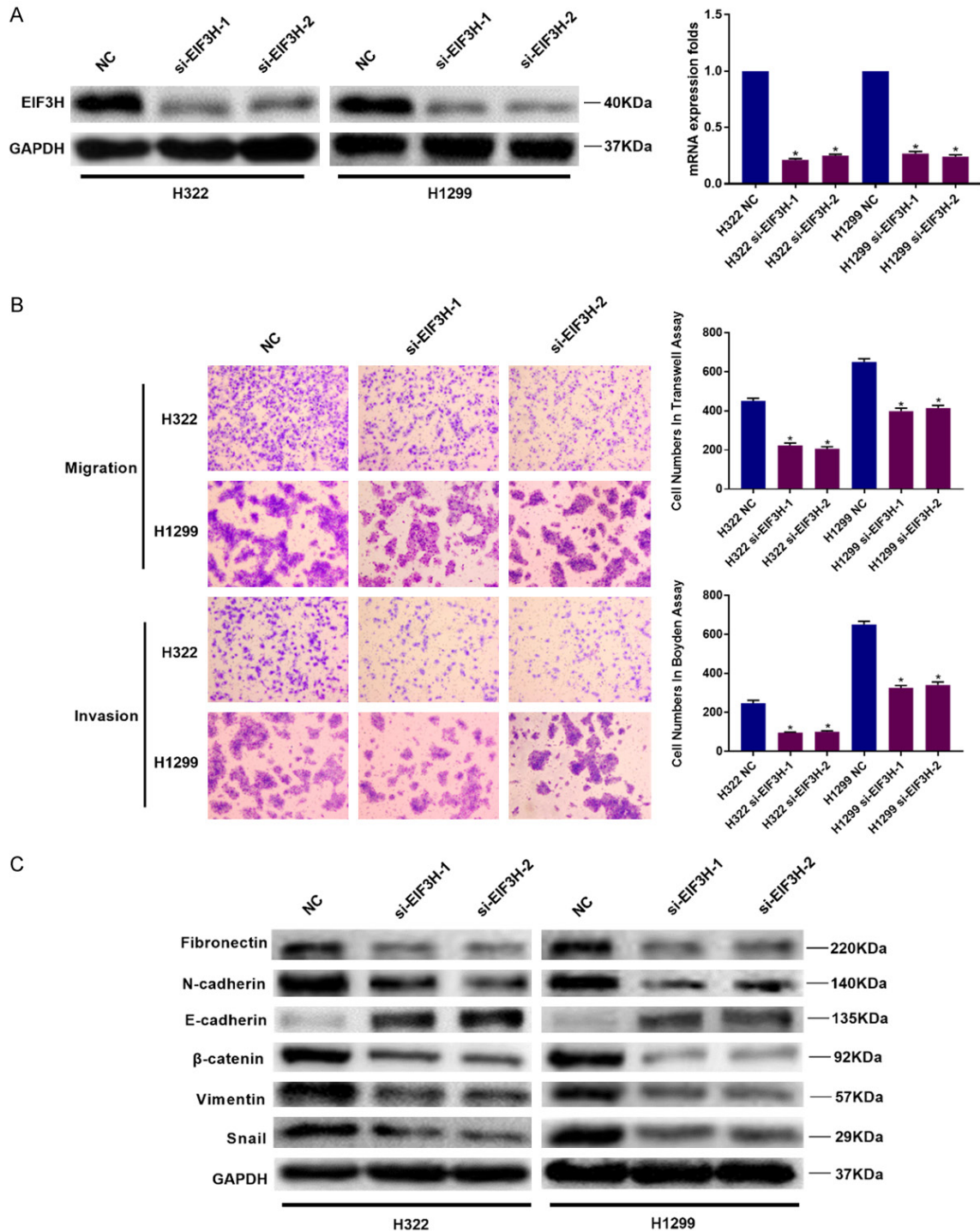
Figure 5. Knockdown of EIF3H attenuates cell migration and invasion by inactivating EMT signals. A. Western blot and RT-qPCR were used to measure the decrease in EIF3H protein and mRNA expression after transfecting siRNA (si-EIF3H-1 or si-EIF3H-2) or the negative control in H322 and H1299 cells. B. Transwell and Boyden assays were used to detect cell migration and invasiveness after EIF3H knockdown. The bar graphs represent the average number of cells that had migrated and invaded through the membranes in three independent experiments. Student's t-test, mean ± S.E., *P<0.05. Scale bar: 100 µm. C. Expression of EMT-related proteins was investigated by Western blot. GAPDH was used as the internal control.

Introduction of PDCD4 in EIF3H-overexpressing LUAD cells abrogated cell migration, invasion and EMT signaling

Our previous experiments showed that PDCD4 suppressed EIF3H expression, but whether EIF3H contributes to the anti-metastatic function of PDCD4 in LUAD remains unknown. After EIF3H overexpression in H322 and H1299 cells, cell migration and invasiveness were enhanced, as shown in transwell and Boyden assays. However, an introduction of PDCD4 by transfection of PDCD4-plasmids into EIF3H-overexpressing cells dramatically reduced EIF3H expression and abrogated its function by inhibiting cell migration and invasion (**Figure 6A**). Meanwhile, increased PDCD4 expression inhibited EMT signaling, which were activated in EIF3H-overexpressed LUAD cells. These results indicated that PDCD4 exerts its anti-metastatic function by inversely regulating EIF3H in LUAD (**Figure 6B**).

Discussion

Local invasion and distant metastasis are the most important biological characteristics of malignant tumors, and are largely responsible for the poor outcomes of patients despite improvements in therapeutic regimens [15-19]. Therefore, it is of great necessity to explore the mechanisms underlying LUAD progression and to identify more effective therapeutic targets. PDCD4 functions as a tumor suppressor gene in various cancers, including lung, colon, renal, ovarian, and breast tumors, due to its critical role in inhibiting cancer cell invasion and metastasis [9, 20-24]. Our study was designed to explore the specific mechanisms of PDCD4's anti-metastatic function in LUAD. After performing CoIP and mass spectrometry, various proteins that potentially interacted with PDCD4 were identified and further analyzed. Among these proteins, we identified EIF3H, a protein translation initiation factor, as an interacting protein of PDCD4.

Eukaryotic translation initiation factor 3 (EIF3) is the largest translation initiation factor. It binds to the 40S ribosomal subunit and interrupts its interaction with the 60S subunit, thus promoting the association of Met-tRNAi with mRNA to start the translational process [25]. It consists of 13 putative subunits, including EIF3H, which is closely related to the pathogenesis of several malignant tumors. EIF3H has been found to be highly amplified and upregulated in breast, prostate, liver, and non-small cell lung cancers [26-28]. Furthermore, amplification of the EIF3H gene was common in metastatic prostate cancer and associated with poor cancer-specific survival in incidentally-found prostate cancer, suggesting it might be functionally involved in tumor progression [29]. In hepatocellular carcinoma, increased EIF3H expression promotes cell growth, colony formation, migration *in vitro*, and xenograft growth *in vivo* [30]. However, the roles of EIF3H in LUAD remain unexplored. We performed further experiments to determine the exact biological function of EIF3H in LUAD. First, EIF3H expression levels were examined by TCGA database mining and IHC detection. Bioinformatics analyses showed that EIF3H was significantly upregulated in LUAD compared with normal lung tissues, and its expression was positively associated with clinical stages, distant metastases, and tumor sizes, as well as a shorter overall survival time (OS) of LUAD patients. We further confirmed the above results by examining EIF3H expression in tissue microarrays by an IHC assay. Consistently, EIF3H expression was increased in LUAD samples, and there were also significant positive relationships between EIF3H expression and clinicopathological features such as clinical stages and T stages. Moreover, in accordance with the results from tissue specimens, elevated EIF3H expression was also detected in 5 LUAD cell lines. Results from *in vitro* experiments suggested that EIF3H significantly promoted migration and invasion of LUAD cells. *In vivo*, it enhanced tumor metastasis in mice. By contrast, knockdown of EIF3H with siRNAs attenuated cancer cell migration and invasion. These aforementioned results revealed that EIF3H promotes metastasis in LUAD, which was consistent with the results in prostate and hepatocellular cancer.

It has been well established that EMT decreases cell adhesion, increases cell motility and promotes metastasis of cells to distant sites. Epithelial cells undergo morphological and biochemical changes into a new mesenchymal phenotype, which results in the downregulation of epithelial markers such as E-cadherin and up-regulation of mesenchymal markers as N-cadherin, vimentin, fibronectin, and snail [31-39]. Our findings demonstrated that activation
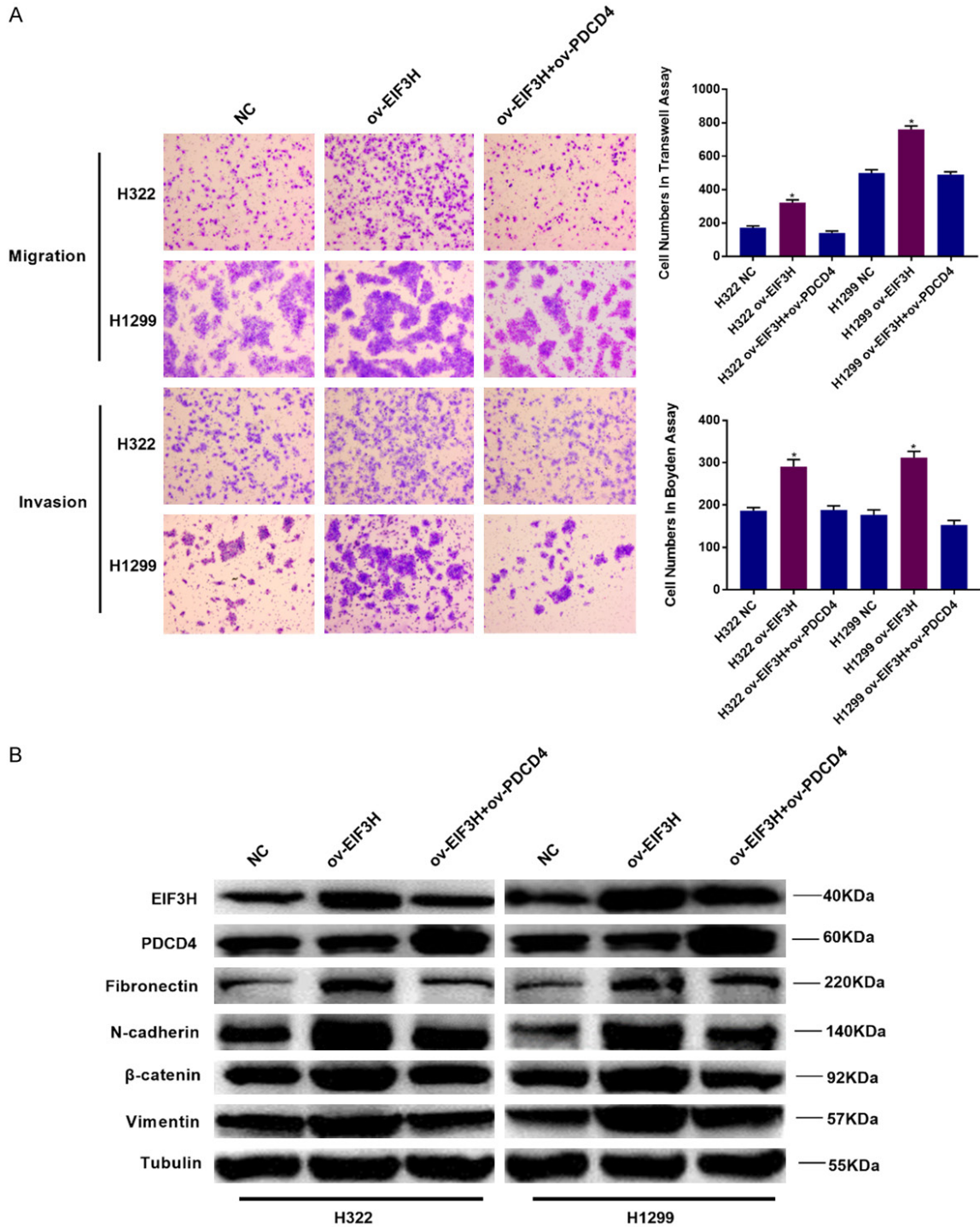
Figure 6. PDCD4 inhibits cell migration and invasion by negatively regulating EIF3H. A. Cell migration and invasion in H322 and H1299 cells transfected with NC, GV358-EIF3H plasmid (ov-EIF3H) or GV358-EIF3H plasmid plus pENTER-PDCD4 plasmid (ov-EIF3H+ov-PDCD4) were examined by transwell and Boyden assays. The bar graphs represent the average number of cells that had migrated and invaded through the membranes in three independent experiments. Student's t-test, mean ± S.E., *P<0.05. Scale bar: 100 μm. B. Expression of EMT-related proteins in the aforementioned cells was detected by Western blot. Tubulin was used as the internal control.

of EMT signaling contributes to the metastasis-promoting function of EIF3H in LUAD.

PDCD4 has been reported to exert its suppressive function by binding to the translation initia-

tion factor EIF4A, thereby preventing the interaction between EIF4A and EIF4G and assembly of mRNA to the 40S ribosome, resulting in the suppression of protein translation. Additionally, PDCD4 inhibits the helicase activity of EIF4A, interrupting the unwinding of stable secondary RNA structures in the 5'-untranslated regions (UTRs) of mRNAs during the translation process [40, 41]. Although PDCD4 inhibited protein synthesis by inactivating EIF4A, the interaction between PDCD4 and EIF3H, as well as their regulatory pattern has never been examined. Therefore, further experiments were carried out to explore the relationship between PDCD4 and EIF3H in LUAD.

Our present study demonstrated that PDCD4 reduced expression of EIF3H in LUAD cells at both the mRNA and protein levels, indicating its transcriptional regulation of EIF3H. Our prior and other previous studies have demonstrated that PDCD4 can suppress the expression of transcription factor c-Jun in various tumors [42, 43]. In this research, c-Jun was showed to bind to the promoter of EIF3H to enhance its transcription. PDCD4 was also found to reduce c-Jun expression and thus repressed EIF3H expression in LUAD cells. These observations indicated that PDCD4 decreased the transcriptional activation of EIF3H by limiting the expression of c-Jun, an oncogenic transcription promoter that increases expression of EIF3H. Moreover, the pattern of EIF3H protein expression in LUAD tissues was opposite to that of PDCD4. Spearman correlation analysis showed a negative expression relation between PDCD4 and EIF3H, which was in accordance with the PDCD4-induced negative modulation of EIF3H in LUAD.

Interestingly, PDCD4 has been widely reported to suppress EMT signaling in various types of cancer [44-46]. Our present study has shown that EIF3H promotes cell migration and invasion in LUAD by activating EMT signaling. Subsequently, PDCD4 was introduced into EIF3H-overexpressing LUAD cells to further investigate the influence of PDCD4 to EIF3H. It demonstrated that increased PDCD4 in EIF3H-overexpressing cells abrogated the migration, invasion, and EMT signaling caused by EIF3H. These results further implied that PDCD4 exerted its anti-metastasis function by negatively modulating EIF3H in LUAD.

In summary, our study suggested EIF3H as a candidate oncogene that promotes cell metastasis by activating EMT signaling in LUAD. Furthermore, this is the first report that PDCD4 suppresses EIF3H by reducing c-Jun-induced transcription, one potential mechanism that contributes to the anti-metastatic activity of PDCD4 in LUAD.

Acknowledgements

Disclosure of conflict of interest

None.

Address correspondence to: Dr. Zhen Liu, Affiliated Cancer Hospital & Institute of Guangzhou Medical University, Guangzhou Municipal and Guangdong Provincial Key Laboratory of Protein Modification and Degradation, State Key Laboratory of Respiratory Disease, School of Basic Medical Sciences, Guangzhou Medical University, Guangzhou 510095, Guangdong, P. R. China. Tel: +86-020-37103236; Fax: +86-020-61650014; E-mail: narcissus_jane@163.com; Dr. Weiyi Fang, Cancer Institute, Southern Medical University, Guangzhou 510515, Guangdong, P. R. China. Tel: +86-020-61650036; Fax: +86-020-61650014; E-mail: fangweiyi1975@163.com

References

[1] Ferlay J, Colombet M, Soerjomataram I, Mathers C, Parkin DM, Piñeros M, Znaor A and Bray F. Estimating the global cancer incidence and mortality in 2018: GLOBOCAN sources and methods. Int J Cancer 2019; 144: 1941-1953.

[2] Bray F, Ferlay J, Soerjomataram I, Siegel RL, Torre LA and Jemal A. Global cancer statistics 2018: GLOBOCAN estimates of incidence and mortality worldwide for 36 cancers in 185 countries. CA Cancer J Clin 2018; 68: 394-424.

[3] Siegel RL, Miller KD and Jemal A. Cancer Statistics, 2017. CA Cancer J Clin 2017; 67: 7-30.

[4] Koo HK, Jin SM, Lee CH, Lim HJ, Yim JJ, Kim YT, Yang SC, Yoo CG, Han SK, Kim JH, Shim YS and Kim YW. Factors associated with recurrence in

patients with curatively resected stage I-II lung cancer. Lung Cancer 2011; 73: 222-229.

[5]   Scagliotti GV and Novello S. Adjuvant therapy in completely resected non-small-cell lung cancer. Curr Oncol Rep 2003; 5: 318-325.

[6]   Stinchcombe TE, Fried D, Morris DE and Socinski MA. Combined modality therapy for stage III non-small cell lung cancer. Oncologist 2006; 11: 809-23.

[7]   Nagao Y, Hisaoka M, Matsuyama A, Kanemitsu S, Hamada T, Fukuyama T, Nakano R, Uchiyame A, Kawamoto M, Yamaguchi K and Hashimoto H. Association of microRNA-21 expression with its targets, PDCD4 and TIMP3, in pancreatic ductal adenocarcinoma. Mod Pathol 2012; 25: 112-121.

[8]   Lankat-Buttgereit B and Goke R. The tumour suppressor Pdcd4: recent advances in the elucidation of function and regulation. Biol Cell 2009; 101: 309-317.

[9]   Allgayer H. Pdcd4, a colon cancer prognostic that is regulated by a microRNA. Crit Rev Oncol Hematol 2010; 73: 185-191.

[10] Schmid T, Jansen AP, Baker AR, Hegamyer G, Hagan JP and Colburn NH. Translation inhibitor Pdcd4 is targeted for degradation during tumor promotion. Cancer Res 2008; 68: 1254-1260.

[11] Jansen AP and Colburn NH. Epidermal expression of the translation inhibitor Pdcd4 suppresses tumorigenesis. Cancer Epidemiol Biomarkers Prev 2005; 14: 2714S-2715S.

[12] Leupold JH, Yang HS, Colburn NH, Asangani I, Post S and Allgayer H. Tumor suppressor Pdcd4 inhibits invasion/intravasation and regulates urokinase receptor (u-PAR) gene expression via Sp-transcription factors. Oncogene 2007; 26: 4550-4562.

[13] Pratheeshkumar P, Son YO, Divya SP, Turcios L, Roy RV, Hitron JA, Wang L, Kim D, Dai J, Asha P, Zhang Z and Shi X. Hexavalent chromium induces malignant transformation of human lung bronchial epithelial cells via ROS-dependent activation of miR-21-PDCD4 signaling. Oncotarget 2016; 7: 51193-51210.

[14] Chen Y, Knösel T, Kristiansen G, Pietas A, Garber ME, Matsuhashi S, Ozaki L and Petersen L. Loss of PDCD4 expression in human lung cancer correlates with tumour progression and prognosis. J Pathol 2003; 200: 640-646.

[15] Dong L, Dong Q, Chen Y, Li Y, Zhang B, Zhou F, Lyu X, Chen GG, Lai P, Kung HF and He ML. Novel HDAC5-interacting motifs of Tbx3 are essential for the suppression of E-cadherin expression and for the promotion of metastasis in hepatocellular carcinoma. Signal Transduct Target Ther 2018; 3: 22.

[16] Li B, Cao Y, Meng G, Qian L, Xu T, Yan C, Luo O, Wang S, Wei J, Ding Y and Yu D. Targeting glutaminase 1 attenuates stemness properties in hepatocellular carcinoma by increas-

ing reactive oxygen species and suppressing Wnt/beta-catenin pathway. EBioMedicine 2019; 39: 239-254.

[17] Lin X, Zuo S, Luo R, Li Y, Yu G, Zou Y, Zhou Y, Liu Z, Liu Y, Hu Y, Xie Y, Fang W and Liu Z. HBX-induced miR-5188 impairs FOXO1 to stimulate β-catenin nuclear translocation and promotes tumor stemness in hepatocellular carcinoma. Theranostics 2019; 9: 7583-7598.

[18] Zhang L, Dong D, Li H, Tian J, Ouyang F, Mo X, Zhang B, Luo X, Lian Z, Pei S, Dong Y, Huang W, Liang C, Liu J and Zhang S. Development and validation of a magnetic resonance imaging-based model for the prediction of distant metastasis before initial treatment of nasopharyngeal carcinoma: a retrospective cohort study. EBioMedicine 2019; 40: 327-335.

[19] Wang S, Zhong L, Li Y, Xiao D, Zhang R, Liao D, Lv D, Wang X, Wang J, Xie X, Chen J, Wu Y and Kang T. Up-regulation of PCOLCE by TWIST1 promotes metastasis in Osteosarcoma. Theranostics 2019; 9: 4342-4353.

[20] Lankat-Buttgereit B and Göke R. The tumour suppressor Pdcd4: recent advances in the elucidation of function and regulation. Biol Cell 2009; 101: 309-317.

[21] Wang Q, Zhu J, Wang YW, Dai Y, Wang YL, Wang C, Liu J, Baker A, Colburn NH and Yang HS. Tumor suppressor Pdcd4attenuates Sin1 translation to inhibit invasion in colon carcinoma. Oncogene 2017; 36: 6225-6234.

[22] Bera A, Das F, Ghosh-Choudhury N, Kasinath BS, Abboud HE and Choudhury GG. microRNA-21-induced dissociation of PDCD4 from rictor contributes to Akt-IKKβ-mTORC1 axis to regulate select renal cancer cell invasion. Exp Cell Res 2014; 328: 99-117.

[23] Wei N, Liu SS, Chan KK and Ngan HY. Tumour suppressive function and modulation of programmed cell death 4 (PDCD4) in ovarian cancer. PLoS One 2012; 7: e30311.

[24] Cuesta R and Holz MK. RSK-mediated downregulation of PDCD4 is required for proliferation, survival, and migration in a model of triple-negative breast cancer. Oncotarget 2016; 7: 27567-27583.

[25] Hershey JW, Asano K, Naranda T, Vornlocher HP, Hanachi P and Merrick WC. Conservation and diversity in the structure of translation initiation factor EIF3 from humans and yeast. Biochimie 1996; 78: 903-7.

[26] Nupponen NN, Isola J and Visakorpi T. Mapping the amplification of EIF3S3 in breast and prostate cancer. Genes Chromosomes Cancer 2000; 28: 203-10.

[27] Okamoto H, Yasui K, Zhao C, Arii S and Inazawa J. PTK2 and EIF3S3 genes may be amplifi-

cation targets at 8q23-q24 and are associated with large hepatocellular carcinomas. Hepatology 2003; 38: 1242-1249.

[28] Cappuzzo F, Varella-Garcia M, Rossi E, Gajapathy S, Valente M, Drabkin H and Gemmill R. MYC and EIF3H Coamplification significantly improve response and survival of non-small cell lung cancer patients (NSCLC) treated with gefitinib. J Thorac Oncol 2009; 4: 472-478.

[29] Saramaki O, Willi N, Bratt O, Gasser TC, Koivisto P, Nupponen NN, Bubendorf L and Visakorpi T. Amplification of EIF3S3 gene is associated with advanced stage in prostate cancer. Am J Pathol 2001; 159: 2089-94.

[30] Zhu Q, Qiao GL, Zeng XC, Li Y, Yan JJ, Duan R and Du ZY. Elevated expression of eukaryotic translation initiation factor 3H is associated with proliferation, invasion and tumorigenicity in human hepatocellular carcinoma. Oncotarget 2016; 7: 49888-49901.

[31] Lin X, Zuo S, Luo R, Li Y, Yu G, Zou Y, Zhou Y, Liu Z, Liu Y, Hu Y, Xie Y, Fang W and Liu Z. HBX-induced miR-5188 impairs FOXO1 to stimulate β-catenin nuclear translocation and promotes tumor stemness in hepatocellular carcinoma. Theranostics 2019; 9: 7583-7598.

[32] Liu Y, Jiang Q, Liu X, Lin X, Tang Z, Liu C, Zhou J, Zhao M, Li X, Cheng Z, Li L, Xie Y, Liu Z and Fang W. Cinobufotalin powerfully reversed EBV-miR-BART22-induced cisplatin resistance via stimulating MAP2K4 to antagonize nonmuscle myosin heavy chain IIA/glycogen synthase 3β/β-catenin signaling pathway. EBioMedicine 2019; 48: 386-404.

[33] Li Y, Liu X, Lin X, Zhao M, Xiao Y, Liu C, Liang Z, Lin Z, Yi R, Tang Z, Liu J, Li X, Jiang Q, Li L, Xie Y, Liu Z and Fang W. Chemical compound cinobufotalin potently induces FOXO1-stimulated cisplatin sensitivity by antagonizing its binding partner MYH9. Sig Transduct Target Ther 2019; 4: 48.

[34] Dong L, Dong Q, Chen Y, Li Y, Zhang B, Zhou F, Lyu X, Chen GG, Lai P, Kung HF and He ML. Novel HDAC5-interacting motifs of Tbx3 are essential for the suppression of E-cadherin expression and for the promotion of metastasis in hepatocellular carcinoma. Signal Transduct Target Ther 2018; 3: 22.

[35] Chen Y, Liu Z, Wang H, Tang Z, Liu Y, Liang Z, Deng X, Zhao M, Fu Q, Li L, Cai H, Xie W and Fang W. VPS33B negatively modulated by nicotine functions as a tumor suppressor in colorectal cancer. Int J Cancer 2020; 146: 496-509.

[36] Zhao M, Xu P, Liu Z, Zhen Y, Chen Y, Liu Y, Fu Q, Deng X, Liang Z, Li Y, Lin X and Fang W. Dual roles of miR-374a by modulated c-Jun respectively targets CCND1-inducing PI3K/AKT signal and PTEN-suppressing Wnt/β-catenin signaling in non-small-cell lung cancer. Cell Death Dis 2018; 9: 78.

[37] Fu Q, Song X, Liu Z, Deng X, Luo R, Ge C, Li R, Li Z, Zhao M, Chen Y, Lin X, Zhang Q and Fang W. miRomics and proteomics reveal a miR-296-3p/PRKCA/FAK/Ras/c-Myc feedback loop modulated by HDGF/DDX5/β-catenin complex in lung adenocarcinoma. Clin Cancer Res 2017; 23: 6336-6350.

[38] Hu M, Guo W, Liao Y, Xu D, Sun B, Song H, Wang T, Kuang Y, Jing B, Li K, Ling J, Yao F and Deng J. Dysregulated ENPP1 increases the malignancy of human lung cancer by inducing epithelial-mesenchymal transition phenotypes and stem cell features. Am J Cancer Res 2019; 9: 134-144.

[39] Li RM, Nai MM, Duan SJ, Li SX, Yin BN, An F, Zhai YQ, Liu J, Chu YR, Yu Y and Song WY. Down-expression of GOLM1 enhances the chemo-sensitivity of cervical cancer to methotrexate through modulation of the MMP13/EMT axis. Am J Cancer Res 2018; 8: 964-980.

[40] Yang HS, Jansen AP, Komar AA, Zheng X, Merrick WC, Costes S, Lockett SJ, Sonenberg N and Colburn NH. The transformation suppressor Pdcd4 is a novel eukaryotic translation initiation factor 4A binding protein that inhibits translation. Mol Cell Biol 2003; 23: 26-37.

[41] Parsyan A, Svitkin Y, Shahbazian D, Gkogkas C, Lasko P, Merrick WC and Sonenberg N. mRNA helicases: the tacticians of translational control. Nat Rev Mol Cell Biol 2011; 12: 235-45.

[42] Zhen Y, Fang W, Zhao M, Luo R, Liu Y, Fu Q, Chen Y, Cheng C, Zhang Y and Liu Z. miR-374a-CCND1-pPI3K/AKT-c-JUN feedback loop modulated by PDCD4 suppresses cell growth, metastasis, and sensitizes nasopharyngeal carcinoma to cisplatin. Oncogene 2017; 36: 275-285.

[43] Cho JH, Kim YW, Choi BY and Keum YS. Sulforaphane inhibition of TPA-mediated PDCD4 downregulation contributes to suppression of c-Jun and induction of p21-dependent Nrf2 expression. Eur J Pharmacol 2014; 741: 247-53.

[44] Yu H, Zeng J, Liang X, Wang W, Zhou Y, Sun Y, Liu S, Li W, Chen C and Jia J. Helicobacter pylori promotes epithelial-mesenchymal transition in gastric cancer by downregulating programmed cell death protein 4 (PDCD4). PLoS One 2014; 9: e105306.

[45] Zhang R and Xia T. Long non-coding RNA XIST regulates PDCD4 expression by interacting with miR-21-5p and inhibits osteosarcoma cell growth and metastasis. Int J Oncol 2017; 51: 1460-1470.

[46] Huo W, Zhao G, Yin J, Ouyang X, Wang Y, Yang C, Wang B, Dong P, Wang Z, Watari H, Chaum E, Pfeffer LM and Yue J. Lentiviral CRISPR/Cas9 vector mediated miR-21 gene editing inhibits the epithelial to mesenchymal transition in ovarian cancer cells. J Cancer 2017; 8: 57-64.